WATER RESOURCES RESEARCH, VOL. 27, NO. 11, PAGES 3009-3017, NOVEMBER 1991

A Note on Transport in Stratified Formations by Flow Tilted With Respect to the Bedding

PAOLO SALANDIN

Istituto di Idraulica "Giovanni Poleni," Università di Padova, Padua, Italy

ANDREA RINALDO

Dipartimento di Ingegneria Civile e Ambientale, Università di Trento, Trento, Italy

GEDEON DAGAN

Department of Fluid Mechanics and Heat Transfer, Faculty of Engineering, Tel Aviv University, Tel Aviv, Israel

The tendency to ergodicity of transport through heterogeneous stratified formations by a flow tilted with respect to the bedding is examined in this note. The idealized model of evenly stratified formations resembles recharge areas in naturally layered sedimentary geological structures over short distances, and transport features of more complex heterogeneous structures. Two cases are considered herein: the ergodic limit and the nonergodic regime. In the former case the theory predicts a constant asymptotic value of longitudinal dispersivity controlled by the log transmissivity integral scale. In the latter case, asymptotic results of an analytic nature are derived for the limit case of large travel times. Monte Carlo simulations are performed to study the plume evolutions for a wide range of heterogeneities and of initial size of the solute body transverse to the bedding. Results are compared with the analytical solution. It is concluded that, in the realistic case of finite initial transverse size of the plumes, ergodicity is not obeyed. Ergodic conditions, in our experiments, were not achieved even for a solute body whose dimension was 400 times the log transmissivity correlation scale. In such cases, theoretical and numerical evidence suggests that in nonergodic regimes the longitudinal dispersion coefficient tends asymptotically to zero for any initial size of the solute body.

1. INTRODUCTION

The dispersive mechanism of transport in aquifers is governed by the spatial variability of the hydraulic conductivity K. One of the simplest models of heterogeneity is that of stratified formations for which K varies only in the vertical direction. Interest in this model has been fostered, on the one hand, by the presence of layering in sedimentary formations and on the other hand, by its simplicity. Although perfect layering over large horizontal distances is an idealization which is quite improbable in nature, the model may apply to flow and transport at short distances. In any case it may serve as a simple tool to grasp the transport phenomenon in more complex heterogeneous structures. No wonder that the stratified model has been the object of numerous studies in the past [e.g., *Mercado*, 1967; *Marle et al.*, 1967; *Gelhar et al.*, 1979; *Matheron and de Marsily*, 1980; *Güven et al.*, 1984; *Güven and Molz*, 1986; *Cvetkovic and Shapiro*, 1989; *Dagan*, 1990]. In most of these studies the flow is assumed to be parallel to the bedding, i.e., it is driven by a constant and horizontal head gradient, J, with velocity given by Darcy's law $V_1 = KJ/n$, where n is the constant effective porosity. In the aforementioned studies, K is assumed to be random. Conversely, if K is regarded as deterministic [e.g., *Marle et al.*, 1967], the concentration is averaged over the formation thickness which in turn is large compared to the heterogeneity scale I. The longitudinal dispersion coefficient D is most conveniently defined by the Aris moments method [*Aris*, 1956] as half of the rate of change of the second spatial moment of the solute body. Under ergodic conditions, implied by most previous studies, D is equal to $\bar{D}$, the ensemble mean of the coefficient of dispersion of a test particle around its mean trajectory. In the sequel we will differentiate among these dispersion coefficients.

Three regimes of transport are present for flow parallel to the layering and for transport of a conservative solute [*Dagan*, 1989]. In the short-time Taylor regime [*Taylor*, 1953] (regime 1) transverse pore-scale dispersion D_d can be neglected and solute particles are convected by V_1, valid for $tD_d/I^2 \ll 1$. In this regime, D grows linearly with the time t [*Mercado*, 1967]. The intermediate *Matheron and de Marsily* [1980] regime (regime 2) is valid for $tD_d/I^2 > 1$ but $tD_d/B^2 \ll 1$, where B is the entire thickness of the aquifer. In this case transverse pore-scale dispersion is effective in ensuring mixing over the layers, but not over the entire thickness B. In their fundamental work, *Matheron and de Marsily* [1980] have shown that D grows like $t^{1/2}$ in this regime. For both regimes 1 and 2 the formation and the solute body may be assumed to be unbounded since the thickness B is immaterial, the only relevant length scale being I. In *Taylor*'s [1953] asymptotic regime (regime 3), $tD_d/B^2 \gg 1$. In this case, transverse pore-scale dispersion ensures mixing over the entire thickness and D tends to a constant value. However, due to the smallness of D_d, for porous media (dispersivity of order of 10^{-3} m) and the large value of $B = O(10^1\text{–}10^2$ m), attaining the third regime is practically impossible. Therefore, unlike flow and transport

Paper number 91WR01937.
0043-1397/91/91WR-01937$02.00

in other regimes, regimes 1 and 2 are the ones of interest in the present context.

Two important features of these two regimes are, first, D increases permanently with the travel time, i.e., no Fickian limit is reached, and secondly, the phenomenon depends crucially on D_d, the transverse pore-scale dispersion.

Matheron and de Marsily [1980] have investigated an additional type of flow, namely, the one driven by a head gradient tilted with respect to the bedding in an unbounded formation. In this case, which may arise in presence of recharge, a small vertical drift of velocity is superimposed upon the horizontal motion. The main finding of *Matheron and de Marsily* [1980] is that the vertical drift of velocity V_2 has a dramatic impact upon transport: (1) unlike in regime 2 above, the dispersion coefficient D, in the direction parallel to the bedding, tends to a constant value for sufficiently large $V_2 t/I$ and (2) this constant D is practically independent of D_d for the large $P_e = V_2 I/D_d$ encountered in practice and D_d can be neglected altogether. Furthermore, D is proportional to the velocity integral scale. Since a constant D characterizes diffusive transport, *Matheron and de Marsily* [1980, p. 911] conclude that "Fickian behavior will take place asymptotically under the very reasonable assumption that the integral of the covariance of the parallel velocity component (or permeability) is finite."

The results can be conveniently interpreted in the framework of the Lagrangian transport theory. Indeed, for flow parallel to the bedding and in regime 1, a particle is convected with constant, random velocity and there is no mechanism to ensure the mixing which leads to a constant D. In contrast, in the presence of drift, each particle spans layers of different K and the conditions of applicability of the central limit theorem may be fulfilled, if many integral scales are covered by the trajectory. The results are illustrated, for instance, by Figure 8*b* of *Matheron and de Marsily* [1980]. Since transport by tilted flow displays features which are encountered in two- or three-dimensional heterogeneous structures, its study is of definite interest.

As we have mentioned above, all the results are underlain by the ergodic hypothesis, i.e., from a theoretical standpoint they are valid for an infinite solute body or for a sufficiently large time to ensure mixing by pore-scale dispersion over the entire thickness. It is tacitly admitted in the literature that ergodic conditions are approached for finite, but sufficiently large plumes as compared with I. Then, the dispersion coefficient D evaluated from the stochastic model applies to any given realization in depicting the rate of change of the second spatial moment of the solute body.

In reality, plumes are of finite size and ergodic conditions may not be obeyed. The uncertainty related to the finite size has been considered for flow parallel to stratification by *Black and Freyberg* [1987] who indicate that it may be quite large. *Dagan* [1989, 1990] examines this issue in a more general context and presents a scheme to define and evaluate the actual effective dispersion coefficient $\bar{D}$, which is random, and the effective dispersion coefficient $\langle \bar{D} \rangle$ defined as the expected value of $\bar{D}$. Furthermore, a framework to evaluate the variance of $\bar{D}$ is also established. Both $\langle \bar{D} \rangle$ and the variance of $\bar{D}$ depend on the solute body size, and ergodicity is assumed to be obeyed for the dimension which is sufficiently large to render the coefficient of variation of $\bar{D}$ close to zero so that $\bar{D} \cong \langle \bar{D} \rangle \cong D$.

To illustrate these ideas, the tendency to ergodicity of transport through stratified formations and tilted flow has been examined, as a project undertaken by a study group at the Summer School of Environmental Dynamics held in June 1990 in Venice (see acknowledgments). The results of Monte Carlo simulations (see section 4) showed to our surprise that ergodic conditions were not achieved even for a solute body whose dimension is 400 times the permeability correlation scale. Furthermore, for large times $\langle \bar{D} \rangle$ tends to zero for any finite size solute body, no matter how large. This and other interesting results have motivated further theoretical elaboration of the problem and its presentation herein.

In section 2 theoretical results obtained under ergodic conditions are described. The results follow *Matheron and de Marsily*'s [1980] approach, simplified along the lines of the presentation of *Dagan* [1989]. In section 3 we examine the nonergodic transport problem along the lines of *Dagan* [1990], while section 4 presents the numerical methodology and section 5 its results. Finally, section 6 discusses the results and their relevance to other transport problems.

2. Transport in Stratified Formations by Flow Tilted With Respect to the Bedding (the Ergodic Limit)

We consider a two-dimensional Cartesian coordinate system with x_1 a horizontal axis and x_2 a vertical one. The hydraulic conductivity $K(x_2)$ is a random function whose statistical moments are given. Furthermore, we assume that K is stationary. Thus, the expected value $\langle K \rangle$ is constant and the covariance $C_K(x_2', x_2'') = \langle K'(x_2')K'(x_2'') \rangle$, with $K' = K - \langle K \rangle$, depends only on $r = |x_2' - x_2''|$. The integral scale I is defined by $I = \int_0^\infty \rho_K(r)\, dr$ where the autocorrelation, ρ_K, is given by $\rho_K = C_K/\sigma_K^2$.

The flow in the x_1 direction is driven by the constant head gradient J such that by Darcy's law

$$V_1(x_2) = U + u(x_2) = JK(x_2)/n \tag{1}$$

where $U = \langle V_1 \rangle = J\langle K \rangle/n$ is constant and $u = JK'/n$ is the residual. The flow domain is regarded as unbounded, and a constant and deterministic vertical velocity V_2 is vectorially added to V_1. Obviously, the velocity field (V_1, V_2) satisfies exactly the continuity equation, and no approximation is involved except for the neglect of influence of boundaries. By virtue of (1), the velocity covariance is given by

$$C_u(x_2', x_2'') = C_u(r) = J^2 C_K(r)/n^2 = s_K^2 U^2 \rho_K(r); \qquad s_K^2 = \sigma_K^2/\langle K \rangle^2 \tag{2}$$

where s_K is the coefficient of variation of K.

Transport is analyzed here by using the Lagrangian methodology (for details see *Dagan* [1989]). With neglect of the effect of pore-scale dispersion, the vectorial equation for the trajectory of a solute particle is $\mathbf{x} = \mathbf{X}(t, a)$, where t is the time. At $t = 0$, $X_1 = 0$, $X_2(0, a) = a$, i.e., the initial location of the particle is $x_1 = 0$, $x_2 = a$. X_1 is a random function determined by the kinematical equation

$$\frac{d\mathbf{X}}{dt} = \mathbf{V}(\mathbf{X}) \tag{3a}$$

that is,

$$\frac{dX_1}{dt} = U + u(X_2); \qquad \frac{dX_2}{dt} = V_2. \tag{3b}$$

Integration of the last equation gives $X_2 = a + V_2 t$ and with the above initial condition X_1 in (3b) becomes

$$X_1(t, a) = Ut + \int_0^t u(V_2 t' + a)\, dt'. \tag{4}$$

The fundamental equation (4) is our starting point. In contrast to (3a), which leads to a stochastic integrodifferential system for **X**, (4) is of considerable simplicity: it expresses X_1 explicitly in terms of u, whereas X_2 is deterministic. Of course, this result pertains to the assumption of perfect layering.

From (4) we have $\langle X_1 \rangle = Ut$, whereas the two-particle covariance $X_{11}(t, a, b) = \langle X_1'(t, a) X_1'(t, b) \rangle$ (defined in words as the covariance at time t of the displacement of two particles whose initial positions are, respectively, $x_2 = a$ and $x_2 = b$ at $t = 0$) is given by

$$X_{11}(t, a, b) = \int_0^t \int_0^t C_u(V_2 t' + a, V_2 t'' + b)\, dt' dt''. \tag{5}$$

In particular, the one-particle variance, for $a = b$, is written as follows:

$$\begin{aligned} X_{11}(t) &= \int_0^t \int_0^t C_u[V_2(t' - t'')]\, dt' dt'' \\ &= 2 \int_0^t (t - t') C_u(V_2 t')\, dt' \\ &= 2 s_K^2 \frac{U^2}{V_2^2} l^2 \int_0^\tau (\tau - \tau') \rho_K(l\tau')\, d\tau' \end{aligned} \tag{6}$$

where $\tau = V_2 t/l$ is a dimensionless time and l is a vertical length scale proportional to the integral scale I. The reduction of the double integral in (5) to a single one is achieved by the change of variables $t' - t'' \to t'$, $t'' \to t''$ and accounting for $C_u(V_2 t') = C_u(-V_2 t')$. This is a particular case of the Cauchy algorithm [*Dagan*, 1989].

For ergodic transport, the dispersion coefficient in the x_1 direction is defined by

$$D(\tau) \doteq \frac{1}{2} \frac{dX_{11}(t)}{dt} = s_K^2 \frac{U^2}{V_2} l \int_0^\tau \rho_K(l\tau')\, d\tau' \tag{7}$$

where the last expression results from (6).

To illustrate these concepts we have represented in Figure 1*a* a few possible trajectories of the ensemble of **X**. Thus X_{11} is a measure of the spread of the trajectories around their mean $\langle X_1 \rangle = Ut$, $X_2 = V_2 t$. It is clear from (7) that if K has a finite integral scale I, it follows that $\int_0^\infty \rho_K(l\tau')\, d\tau' = I/l$ and $D(\infty) = s_K^2 U^2 I/V_2$, a result obtained by *Matheron and de Marsily* [1980].

To further illustrate the results, we select now a model of formation constituted by layers of constant thickness l with K generated independently from a lognormal population $Y = \ln K$, with $\langle Y \rangle$ and σ_Y^2 the expected value and variance, respectively. In this case, and assuming that both K values and the location of interfaces between layers are random to ensure stationarity, we have

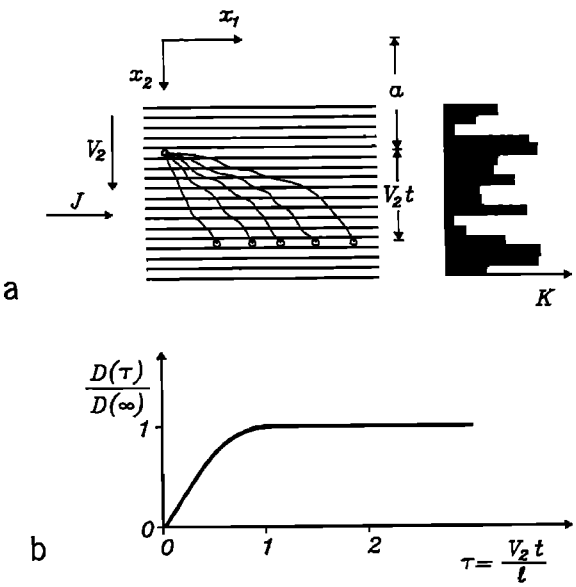

Fig. 1. (*a*) Sketch of a few realizations of one-particle trajectories. (*b*) The dependence of the dispersion coefficient D upon time (equation (9)).

$$\begin{aligned} s_K^2 &= \frac{\sigma_K^2}{\langle K \rangle^2} = e^{\sigma_Y^2} - 1; \\ \rho_K &= 1 - \frac{|r|}{l} \qquad |r| < l, \\ \rho_K &= 0 \qquad |r| > l. \end{aligned} \tag{8}$$

Hence, we obtain from (7)

$$\begin{aligned} D(\infty) &= \frac{U^2}{V_2} (e^{\sigma_Y^2} - 1) \frac{l}{2}; \\ \frac{D(\tau)}{D(\infty)} &= 2\tau \left(1 - \frac{\tau}{2}\right) \qquad \tau < 1; \\ \frac{D(\tau)}{D(\infty)} &= 1 \qquad \tau > 1 \end{aligned} \tag{9}$$

and $D(\tau)/D(\infty)$ is represented in Figure 1*b*.

Under ergodic conditions, i.e., for a solute body extending vertically over an infinite number of integral scales, it is assumed that ensemble and space averages may be exchanged. Then the centroid of the solute body moves along the mean **X** whereas the rate of change of its second spatial moment around the centroid is equal to $2D$.

3. Transport in Stratified Formations by Flow Tilted With Respect to the Bedding (the Nonergodic Regime)

We consider now a solute body whose initial shape is a slab of zero thickness in the x_1 direction, lying along the segment $0 < x_2 < L$ (Figure 2). The thickness in the x_1

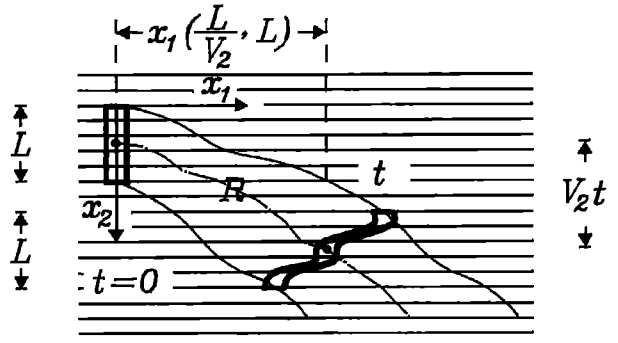

Fig. 2. Initial solute body and solute body at time t.

direction is immaterial since any slab parallel to the x_1 axis just translates with velocity $(V_1(x_2), V_2)$.

With $C(\mathbf{x}, t)$ the concentration field, the first three spatial moments of the solute body are defined by

$$M = \int nC\, d\mathbf{x}; \qquad \mathbf{R} = \frac{1}{M}\int nC\mathbf{x}\, d\mathbf{x};$$
$$S_{ij} = \frac{1}{M}\int nC(x_i - R_i)(x_j - R_j)\, d\mathbf{x} \qquad i, j = 1, 2, \tag{10}$$

where M is the total mass (constant for a conservative solute), $\mathbf{R}$ is the vectorial coordinate of the centroid and the S_{ij} are proportional to the moments of inertia of the solute body. We assume that the solute mass is uniformly distributed within the slab. Then we get for the two moments of interest [*Dagan*, 1990]

$$R_1(t) = \frac{1}{L}\int_0^L X_1(t, a)\, da;$$
$$S_{11} = \frac{1}{L}\int_0^L [X_1(t, a) - R_1(t)]^2\, da. \tag{11}$$

R_1 and S_{11} are random variables and can be estimated in terms of their statistical moments. Starting with R_1 in (11) we have by (4) and (5)

$$\langle R_1\rangle = \frac{1}{L}\int_0^L \langle X_1\rangle\, da = Ut$$

$$R_{11} = \mathrm{Var}\,(R_1) = \frac{1}{L^2}\int_0^L\int_0^L X_{11}(t, a, b)\, da\, db \tag{12}$$

$$= \frac{1}{L^2}\int_0^L\int_0^L\int_0^t\int_0^t C_u[V_2(t' - t'') + a - b]\, da\, db\, dt'\, dt''.$$

By the changes of variables $a - b \to a$, $b \to b$ and $t' - t'' \to t'$, $t'' \to t''$ in (12) the quadruple integral can be reduced to a double one as follows:

$$R_{11}(t, L) = \frac{2}{L^2}\int_0^L\int_0^t (t - t')(L - a)$$
$$\cdot [C_u(V_2t' + a) + C_u(V_2t' - a)]\, dt'\, da$$
$$= 2s_K^2\frac{U^2}{V_2^2}\frac{l^2}{\lambda^2}\int_0^\lambda\int_0^\tau (\tau - \tau')(\lambda - \alpha)$$
$$\cdot [\rho_K(l\tau' + l\alpha) + \rho_K(l\tau' - l\alpha)]d\tau'\, d\alpha \tag{13}$$

where $\tau = V_2t/l$, $\lambda = L/l$ and $\alpha = a/l$ are dimensionless variables. The passage to the last expression in (13) is similar to that of (6). Equation (13) permits one to calculate the variance of the centroid coordinate for any given ρ_K. Asymptotically, we get for a fixed λ and for $\tau \gg I/l$ and $\tau \gg \lambda$

$$\int_0^\tau [\rho_K(l\tau' + l\alpha) + \rho_K(l\tau' - l\alpha)]\, d\tau' \to 2\frac{I}{l}$$
$$R_{11} \to 2s_K^2\frac{U^2}{V_2^2}lI\tau. \tag{14}$$

In contrast, for a fixed τ but for $\lambda \gg 1$ and $\lambda \gg \tau$, we obtain in (13)

$$\int_0^\tau [\rho_K(l\tau' + l\alpha) + \rho_K(l\tau' - l\alpha)]\, d\tau' \to 2\frac{I}{l}$$
$$R_{11} \to 2s_K^2\frac{U^2}{V_2^2}\frac{lI}{\lambda}\tau^2. \tag{15}$$

The coefficient of variation s_R, equal to $R_{11}^{1/2}/\langle R_1\rangle = R_{11}^{1/2}/(Ut)$, is seen to tend to zero either for $\lambda = L/l \to \infty$ for a fixed $\tau = tV_2/l$ or for $\tau \to \infty$ and a fixed λ. The asymptotic expressions of s_R, based on (14) and (15), are as follows:

$$s_R \to \left(\frac{2I}{l}\right)^{1/2} s_K\tau^{-1/2} \qquad \tau \to \infty,\ \lambda \text{ fixed};$$
$$s_R \to \left(\frac{2I}{l}\right)^{1/2} s_K\lambda^{-1/2} \qquad \lambda \to \infty,\ \tau \text{ fixed}. \tag{16}$$

Regarding $s_R \cong 0$ as a criterion of ergodicity for the centroid motion, it is seen that it is ensured for any time only if $L/I \gg 1$. In section 4 we shall describe the results of Monte Carlo simulations for equal-thickness layers, for which $l = 2I$ and $s_K^2 = \exp(\sigma_Y^2) - 1$. An important point, however, is that R_{11} itself (equation (14)) is growing linearly with t for any given L.

We discuss next the quantity of major interest, namely, S_{11} in (11). Under nonergodic conditions it is a random variable since in each realization, like the one depicted in Figure 2, it has a different value.

Following *Dagan* [1990] we define first the actual dispersion coefficient by $\bar{D} = \frac{1}{2}(dS_{11}/dt)$, a measure of the spread of the solute body around its centroid in each realization. $\bar{D}$ is random and subject to uncertainty and it is only appropriate to define the effective dispersion coefficient by $\langle\bar{D}\rangle = \frac{1}{2}(d\langle S_{11}\rangle/dt)$, the best estimate of $\bar{D}$.

The fundamental relationship satisfied by $\langle S_{11}\rangle$ [*Kitanidis*, 1988; *Dagan*, 1989] is as follows:

$$\langle S_{11}(t, L)\rangle = S_{11}(0, L) + X_{11}(t) - R_{11}(t, L) \tag{17a}$$

that is,

$$\langle \bar{D}(t, L)\rangle = \frac{1}{2}\frac{d\langle S_{11}\rangle}{dt} = D(t) - \frac{1}{2}\frac{dR_{11}(t, L)}{dt}. \quad (17b)$$

This relationship has a simple interpretation: X_{11}, the expected value of the spatial moment with respect to the mean centroid location, is equal to $\langle S_{11}\rangle$, the variance with respect to the actual centroid, augmented by R_{11}, the variance of R_1.

It is seen that for a solute body of finite dimension L the effective dispersion coefficient (equation (17)) depends on L. It is only for $L/I \to \infty$ that dR_{11}/dt in (17b) tends to zero and the ergodic relationship $\langle \bar{D}\rangle = D$ is satisfied.

We are now in a position to compute $\langle \bar{D}\rangle$ in (17b) by using the previous results. Indeed, from (7) and (13), we get

$$\langle \bar{D}(t, L)\rangle = s_K^2 \frac{U^2}{V_2}\frac{l}{\lambda^2}\int_0^\lambda \int_0^\tau (\lambda - \alpha)[2\rho_K(l\tau') - \rho_K(l\tau' + l\alpha) - \rho(l\tau' - l\alpha)]\, d\tau'\, d\alpha. \quad (18)$$

Once again $\langle \bar{D}(t, L)\rangle$ can be evaluated explicitly for any given ρ_K and it is presented in section 4 for the uniform thickness layer formation. It is easy to compute the asymptotic limit of $\langle \bar{D}\rangle$ for large τ and fixed $\lambda = L/l$. Indeed, it is easy to ascertain that for any $\rho_K(r)$ the integral over τ' of $[2\rho_K(l\tau') - \rho_K(l\tau' + l\alpha) - \rho_K(l\tau' - l\alpha)]$ tends to zero as $\tau \to \infty$ and we arrive at the somewhat unexpected result that $\langle \bar{D}(t, L)\rangle \to 0$ for fixed L and $t \to \infty$. This means that transport is never ergodic for a finite size solute body, no matter how large, if enough time elapses. In contrast, for a fixed t but for $\lambda \to \infty$ it is seen that $\langle \bar{D}\rangle \to D$ since dR_{11}/dt in (17) tends to zero. Since in any conceivable application L is finite we conclude that for this type of formation and flow the solute body does not expand in the mean if pore-scale dispersion is neglected.

Since $\langle \bar{D}\rangle \to 0$ for $t \to \infty$ it is worthwhile to evaluate $\langle S_{11}\rangle$ at the same limit. Integration of (18) over t yields

$$\langle S_{11}\rangle = 2s_K^2 \frac{U^2}{V_2^2}\frac{l}{\lambda^2}\int_0^\lambda \int_0^\tau (\lambda - \alpha)[2\xi_K(l\tau') - \xi_K(l\tau' + l\alpha) - \xi_K(l\tau' - l\alpha)]\, d\tau'\, d\alpha \quad (19)$$

$$\xi_K(r) = \int_0^r \rho_K(r')\, dr'.$$

For $\tau \to \infty$ we have $\int_0^\infty \xi_K(l\tau' + l\alpha)\, d\tau' = \int_\alpha^\infty \xi_K(l\tau')\, d\tau'$ and similarly for other integrals. Hence, we obtain in (19)

$$\langle S_{11}(t, L)\rangle \to 4s_K^2 \frac{U^2}{V_2^2}\frac{l}{\lambda^2}\int_0^\lambda (\lambda - \alpha)\int_0^\alpha \xi_K(l\tau')\, d\tau'\, d\alpha \quad (20)$$

$$\tau \to \infty.$$

Finally, to illustrate the results we have evaluated $\langle S_{11}\rangle$ for lognormal K and for layers of uniform thickness, i.e., with ρ_K and s_K as in (8). The final result for $\lambda > 1$ in (20) becomes

$$\langle S_{11}(\infty, L)\rangle = 4\frac{U^2}{V_2^2} l^2 [\exp(\sigma_Y^2) - 1] \cdot \left[\frac{\lambda}{12} - \frac{1}{12} + \frac{1}{24\lambda} - \frac{1}{120\lambda^2}\right]. \quad (21)$$

The striking result is that $\langle S_{11}\rangle$ tends to a constant value, i.e., in the mean and asymptotically a solute body of finite extent does not expand around its centroid. Furthermore, $\langle S_{11}\rangle$ increases with permeability variability, with the integral scale $I = l/2$ and with L, the vertical extent of the solute body.

This main result of the analysis can be understood by inspecting Figure 2. Indeed, let $X_1(t, 0)$ be the trajectory of the highest point of the solute body. The trajectory of any other particle is given by

$$X_1(t, a) = X_1(t, 0) + X_1\left(\frac{a}{V_2}, 0\right) \qquad (0 < a < L) \quad (22)$$

and in particular the lowest particle moves along $X_1(t, L)$. It is seen, therefore, that trajectories of various particles become correlated after a time interval L/V_2 and the solute body moves in a "channel" of constant width $X_1(L/V_2, 0)$ for $t > L/V_2$ (Figure 2). Since $X_1(L/V_2, 0)$ is random, this width differs from realization to realization and S_{11} is a random variable whose variance can be calculated along the same lines (see developments in the work by *Dagan* [1990] for normal X). However, the analytical computations become cumbersome and are left to numerical simulations (section 4).

4. Monte Carlo Simulations of Transport in Layered Formations

The numerical experiments are based on a discretization of the layered aquifer and the solute body as illustrated in Figure 3. The constant thickness of the layers is l. The permeability K, constant for each layer, is supposed to be lognormally distributed and the mean velocity field in the horizontal direction is $U = J\langle K\rangle/n$. In the vertical direction a constant drift of velocity $V_2 = (1/10)U$ is assumed.

A Monte Carlo (MC) method is applied as follows. For each successive iteration a realization is drawn at random from a cumulative normal distribution of log transmissivity $Y = \ln K$, i.e., $P(Y; \langle Y\rangle, \sigma_Y^2)$ (of assigned mean $\langle Y\rangle$ and variance σ_Y^2). This simply implies generating a sequence of random numbers W_i in (0, 1) drawn from a uniform distribution and solving for the ith layer the equation $Y_i = P^{-1}(W_i; \langle Y\rangle, \sigma_Y^2)$.

At time $t = 0$ a rectangular initial solute body of dimension L normal to the layers and of unit width in the direction parallel the bedding (Figure 3) is inserted in the formation. With neglect of pore-scale dispersion, each slug moves by l along x_2 during a period $\Delta t = l/V_2$ and longitudinally by $\Delta x_1 = V_1 \Delta t$ according to the velocity V_1 of the actual layer. For each MC realization we compute the position of the center of mass and the second spatial moment of the solute body moving in the aquifer at the same prefixed time intervals. By repeating this procedure for an arbitrary number of different realizations of $Y(x_2)$ with same mean and variance, one can calculate the statistics (mean and variance) of the two moments of interest over the various realizations.

The horizontal spatial step is generally given by

$$(\Delta X)_{i,p,m} = \frac{J}{n}(K)_{i,p,m}\Delta t = \frac{J}{n}\frac{l}{V_2}(K)_{i,p,m} \quad (23)$$

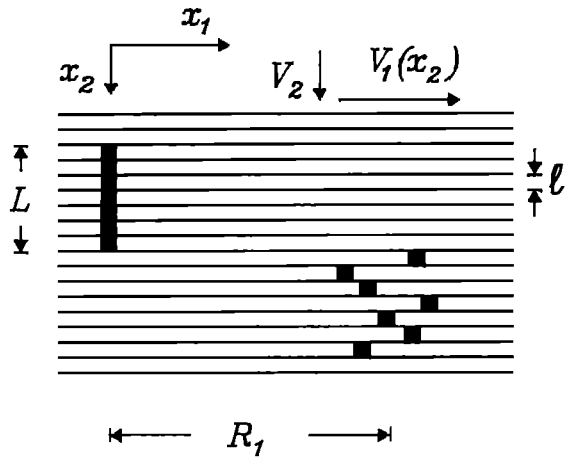

Fig. 3. Definition sketch of the discretized solute body shape for transport in stratified formations by flow tilted with respect to the bedding.

where the index i refers to the ith layer in the initial slug (i = 1, NL), m refers to the mth Monte Carlo run (m = 1, NMC) and p refers to current time which equals the number of crossed layers (p = 1, NTS). Here NL is the number of layers covered by the initial solute body, i.e., NL = L/l, NTS is the number of time steps simulated for each realization, and NMC is the number of different realizations generated by the Monte Carlo simulation.

The position of the center of mass and the second spatial moment at current time $T\Delta t$ (note that T in the discrete stepping procedure is an integer) are given by

$$(R_1(T))_m = \frac{1}{\mathrm{NL}} \sum_{i=1}^{\mathrm{NL}} \sum_{p=1}^{T} (\Delta X)_{i,p,m} = \frac{1}{\mathrm{NL}} \sum_{i=1}^{\mathrm{NL}} (X_i(T))_m$$

$$(S_{11}(T))_m = \frac{1}{\mathrm{NL}} \sum_{i=1}^{\mathrm{NL}} [(X_i(T))_m - (R_1(T))_m]^2 \tag{24}$$

The expected value and the variance of R_1 and S_{11}, over a number NMC of MC runs, are given by

$$\langle R_1(T) \rangle = \frac{1}{\mathrm{NMC}} \sum_{m=1}^{\mathrm{NMC}} (R_1(T))_m$$

$$R_{11}(T) = \mathrm{Var}\,[R_1(T)] = \frac{1}{\mathrm{NMC}} \sum_{m=1}^{\mathrm{NMC}} [(R_1(T))_m - \langle R_1(T) \rangle]^2 \tag{25}$$

and

$$\langle S_{11}(T) \rangle = \frac{1}{\mathrm{NMC}} \sum_{m=1}^{\mathrm{NMC}} (S_{11}(T))_m$$

$$\mathrm{Var}\,[S_{11}(T)] = \frac{1}{\mathrm{NMC}} \sum_{m=1}^{\mathrm{NMC}} [(S_{11}(T))_m - \langle S_1(T) \rangle]^2 \tag{26}$$

respectively.

The numerical experiments assumed four different values of σ_Y^2, equal to 0.5, 1.0, 1.5 and 2.0 respectively. For each value of σ_Y^2 the initial body dimension NL is set equal to 5, 20, 50 and 200. The constant number of time steps NTS is 200.

In all MC method applications a fundamental parameter is the number of runs. The question is, How many realizations are needed to ensure a good approximation for the statistical moments? A parameter of interest to define practical limits is the rate of convergence of a given simulation. It is defined by an estimate of rate of change of the overall deviations of all computed values of a quantity of interest (either R_1 or S_{11}) with increasing MC runs. In order to choose a value for NMC suitable for our purposes (not too large in order to limit the computational burden, although large enough to ensure stable results) several runs have been performed in which the convergence rate of the variances of R_1 and S_{11} as a function of the number of Monte Carlo runs has been studied. The results are illustrated in Figures 4*a* and 4*b*, here plotted in the case λ = 5 and σ_Y^2 = 2 and somewhat arbitrarily normalized. From Figure 4*a* it is inferred that for NMC = 50,000 the results are to be considered stable for the coefficient of variation of R_1. Numerical difficulties arise in computing the time evolution for the coefficient of variation of S_{11} for high values of σ_Y^2 and small values of λ (Figure 4*b*). Nevertheless, we observe that the time-averaged values of the coefficient of variation of S_{11} are near to stabilization. Since the higher statistical moments exhibit a slower velocity of convergence, it is concluded that this number of Monte Carlo runs offers a good balance of accuracy of results and computer run time. Therefore all the results discussed in the next section have been obtained using 50,000 MC runs.

5. Results of the Monte Carlo Simulations

Figure 5 illustrates the time evolution of the coefficient of variation of the centroid trajectory $(R_{11})^{1/2}/\langle R_1 \rangle$ for different values of $\lambda = L/l$ and σ_Y^2. The results are normalized by a factor $(\zeta - 1)^{1/2}$, where $\zeta = \exp(\sigma_Y^2)$. According to (16) this transformation renders the coefficients s_R independent of σ_Y^2 such that at the same value of λ all the curves coincide. We also observe that the larger the number of layers occupied by the initial solute body, the smaller the coefficient of variation that results from the calculations. As we expected theoretically (equation (16)), the variance of the centroid tends to zero for $\lambda \to \infty$ (fixed t) or for large travel times ($tV/2l \to \infty$, fixed λ). This is valid asymptotically with convergence proportional to $\lambda^{-1/2}$ and $\tau^{-1/2}$. For $\lambda \simeq \tau$ and $\lambda \ll 200$, the behavior of the coefficient of variation may differ significantly from the asymptotic values (equation (16)). We note that for λ = 5 the differences between the first limit in (16) and our numerical results at τ = 200 are negligible. Also the second asymptotic result in (16) is confirmed for $\tau \ll \lambda$. From Figure 5 one may also study the tendency to ergodicity in the numerical experiments upon comparison with (17). With reference to other transport problems, it is also of definite interest that heterogeneity is manifested in the uncertainty of the centroid position, the cases of three-dimensional flow being more involved but essentially similar [*Dagan*, 1991].

Figure 6*a* shows the time evolution of the coefficient of variation of S_{11} obtained by dividing $[\mathrm{Var}\,(S_{11})]^{1/2}$ by the

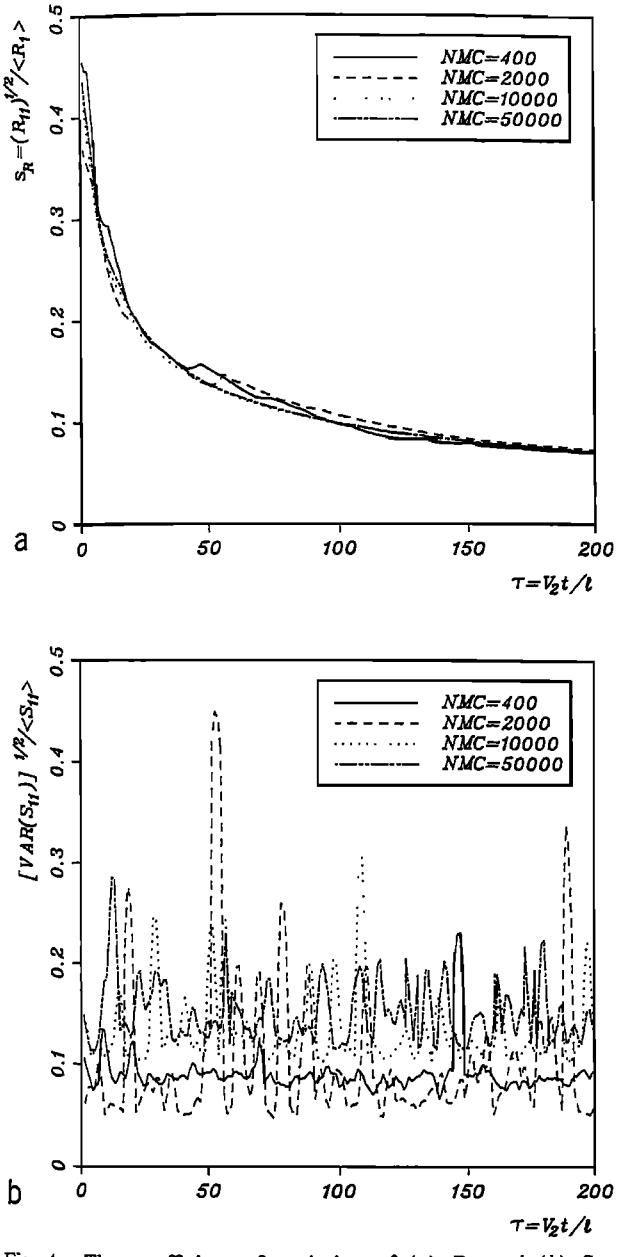

Fig. 4. The coefficient of variation of (*a*) R_1 and (*b*) S_{11}, normalized with respect to σ_Y^2, versus dimensionless time for fixed $\sigma_Y^2 = 2$ and $\lambda = L/l = 5$ as a function of MC runs.

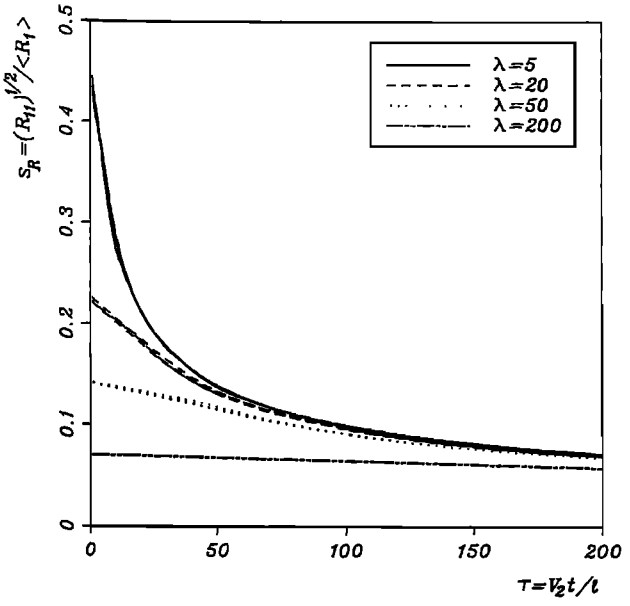

Fig. 5. The coefficient of variation of the centroid trajectory for different σ_Y^2 (= 0.5, 1.0, 1.5 and 2.0) and $\lambda = L/l$ (= 5, 20, 50 and 200) normalized by the quantity $(\zeta - 1)^{1/2}$, where $\zeta = \exp(\sigma_Y^2)$.

asymptotic result of (20), $\langle S_{11}(\infty, L)\rangle$, for various sizes λ of the initial plume and σ_Y^2. The oscillating values of Var (S_{11}) in time affect the corresponding values of the coefficient of variation. To grasp some average features, mean values have been taken over time for the final 15 intervals and are plotted in Figure 6*b*. This is a correct procedure for all cases in which we consider a dimension of the initial solute body $\lambda <$ 200, because when the body has traveled a number of layers equal to λ, the quantities Var (S_{11}) and S_{11} exhibit an oscillating trend about constant mean values. For the cases in which $\lambda = 200$ we consider the results at the end of the modeled period, since the quantities are still growing at $\tau =$ 200. Figure 6*b* suggests that prediction of S_{11} is quite uncertain. As expected, when the initial dimension of the solute body increases the coefficient of variation of S_{11} decreases. However, even when the initial size of the solute body is large, uncertainty remains noteworthy.

Figure 7 compares the ratio of the actual computed values of the longitudinal variance $\langle S_{11}\rangle$ and the theoretical limit (equation (21)) for the various cases investigated. We note that for large travel times all values converge to the theoretical limit except for oscillations. All simulations collapse on a unique curve for the same values of λ but different values of σ_Y^2. We also note that at larger values of λ a slower convergence to the asymptotic value is achieved. The differences from the ergodic results of *Matheron and de Marsily* [1980] are manifest: For any finite initial size of solute body the growth is limited and after an initial development the size of the body remains constant.

Figure 8 illustrates the evolution of the dimensionless dispersion coefficient, defined as the ratio of the effective dispersion coefficient $\langle \bar{D}\rangle = \frac{1}{2} d\langle S_{11}\rangle/dt$ and the value of $D(\infty)$ in (9). Actual values have been obtained by numerical differentiation of the variance $\langle S_{11}\rangle$ of Figure 6. We observe that the dispersion coefficient grows from zero to a maximum and then drops again to zero, at a slower rate for an increasing initial transverse dimension of the solute body. The growth period is confined to an initial stage for which $V_2 t/l < 1$ for which no details can be provided by the present method if of interest. Oscillations in the estimate of variance are enhanced here because of numerical differentiation.

From Figures 5–8 we observe that in transport of solutes in idealized stratified systems by a tilted flow, the solute body does not disperse at all asymptotically no matter how large the log transmissivity correlation scale is. Hence, in view of the theoretical results of section 2, this case of transport is nonergodic for any finite size of the initial solute body. We infer that heterogeneity is manifested in the uncertainty of the centroid position rather than in dispersion, the rate of change of X_{11} in (17*a*) being compensated by that of R_{11}.

These results also bear implications on the behavior of the effective longitudinal dispersivity for more complex structures or for rectangular bodies of finite dimensions, say, l_1, l_2. *Dagan* [1991] discusses in detail the cases of transport in

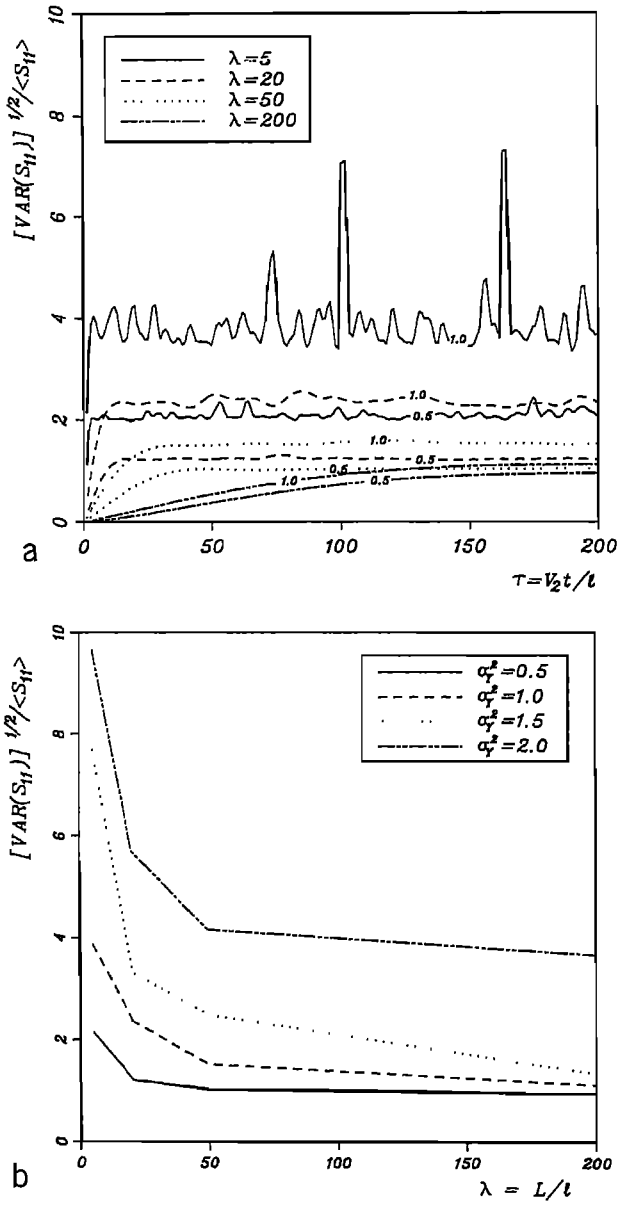

Fig. 6. (*a*) The coefficient of variation of S_{11} for σ_Y^2 equal to 0.5 and 1.0, and $\lambda = L/l$ (5, 20, 50 and 200) versus dimensionless time. Values for σ_Y^2 equal to 1.5 and 2.0 are not included as they are out of scale. (*b*) The asymptotic values averaged over 15 time intervals of the same quantities versus λ.

two-dimensional aquifers of thin solute bodies (1) streamline aligned, and (2) normal to the mean flow. Conclusions similar to those suggested here were drawn in the case of transport of a thin solute body aligned with the mean flow direction.

6. Summary and Conclusions

In the present note we have examined transport in heterogeneous stratified porous formations by a flow tilted with respect to the bedding, for which the theory predicts that, if ergodicity is obeyed, a constant asymptotic value is reached by longitudinal dispersivity. We have proved that in the realistic case of finite transverse sizes of the initial plume, the ergodic requirements are not met. Our methodology is of analytic nature, for a few statistical moments of the solute body, and numerical, based on Monte Carlo simulation of

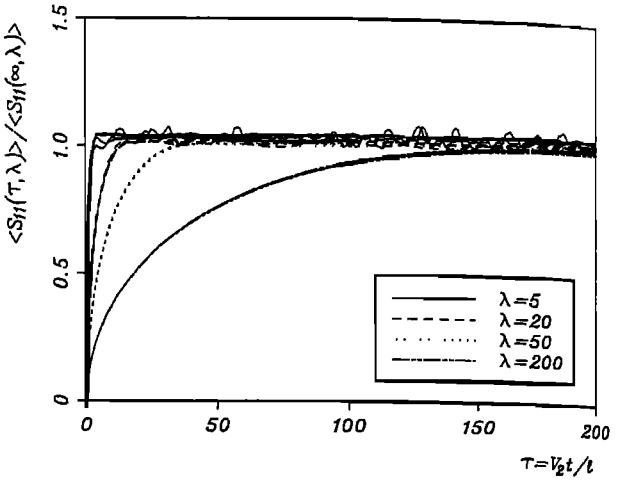

Fig. 7. The ratio between the Monte Carlo simulations results for $\langle S_{11}(\tau, \lambda)\rangle$ and the theoretical $\langle S_{11}(\infty, \lambda)\rangle$ (equation (21)) for different σ_Y^2 (0.5, 1.0, 1.5 and 2.0) and $\lambda = L/l$ (5, 20, 50 and 200).

50,000 realizations of independent lognormally distributed permeabilities of the layers. Our main results are as follows.

1. The centroid of a solute body of finite size moves in a given realization along a sinuous path. However, as shown in Figure 5, this path does not depart too much from the mean one, except at short times and for small plumes.

2. The second spatial moment, a measure of the spread around the centroid, does increase with the travel distance till the latter becomes equal to the vertical extent of the solute body, as illustrated by Figure 7. Subsequently it remains constant, contrary to the linear growth prevailing under ergodic conditions. This result can be simply explained by the tunneling effect displayed in Figure 2: The trailing edge of the solute body moves on a trajectory parallel to that of the leading edge once it has covered a distance equal to the plume vertical extent. Obviously, the presence of the hitherto neglected pore-scale dispersion changes this result, but its effect is often negligible [*Dagan*, 1989].

3. Under these circumstances the "macrodispersion" of effective dispersion coefficient is not a useful entity. In particular, the macrodispersion coefficient tends to zero for sufficiently large travel distance, as illustrated by Figure 8.

4. The prediction of the second spatial moment by the statistical theory is affected by a large degree of uncertainty (see Figure 6*b*).

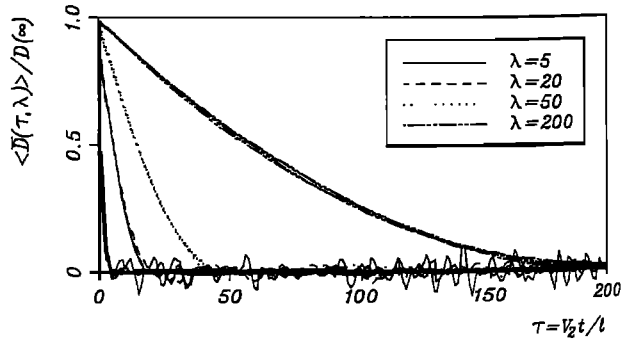

Fig. 8. The ratio between the "effective dispersion coefficient" $\langle \bar{D} \rangle = \frac{1}{2}(d\langle S_{11}\rangle\, dt)$ and $D(\infty)$ (equation (9)). $\langle \bar{D} \rangle$ has been obtained by numerical differentiation of $\langle S_{11}(\tau, \lambda)\rangle$ of Figure 7.

The present study has illustrated a few aspects of transport through heterogeneous formations by employing a simple, but illuminating, example. The salient question is whether similar results apply to the more common type of formations of two- or three-dimensional heterogeneous structures. Recent investigations [*Dagan*, 1991] suggest that the present results apply to transport of thin plumes, aligned with the mean flow direction. In contrast, solute bodies of large transverse dimensions with respect to the heterogeneity scale may disperse according to the ergodic theory.

NOTATION

a initial position of the transported particle.
B thickness of the entire aquifer.
$C(\mathbf{x}, t)$ solute concentration field.
$C_X(\mathbf{r})$ covariance function of the random field X, here assumed stationary, i.e., dependent only on the separation vector $\mathbf{r}$.
D_d pore-scale dispersion coefficient.
$D=\frac{1}{2}\, dX_{11}/dt$, longitudinal dispersion coefficient under ergodic assumptions.
$\bar{D}=\frac{1}{2}\, dS_{11}/dt$, actual effective dispersion coefficient.
$\langle \bar{D} \rangle=\frac{1}{2}\, d\langle S_{11}\rangle/dt$, effective dispersion coefficient.
I correlation (integral) scale of hydraulic conductivity.
J constant head gradient.
K hydraulic conductivity of the porous formation.
l constant thickness of the layers.
L transverse dimension of the initial solute body.
$M=\int C\, d\mathbf{x}$, total solute mass (constant for a conservative solute).
n effective porosity.
NL number of layers covered by the initial plume.
NMC number of Monte Carlo runs.
NTS number of steps in each MC simulation.
$Pe=V_2 I/D_d$, Peclet number.
$r=|x' - x''|$, separation vector between two points x', x''.
$\mathbf{R}=\int C\mathbf{x}\, d\mathbf{x}$, vectorial coordinate of the centroid of the solute body.
R_1 position of the centroid of the solute plume in the longitudinal direction.
R_{11} variance of R_1.
$s_X=\sigma_X/\langle X\rangle$, coefficient of variation of the random field X.
$S_{ij}=1/M \int C(x_i - R_i)(x_j - R_j)\, d\mathbf{x}$, variance of the solute body.
t current time.
T number of time steps Δt.
u velocity fluctuation with respect to the mean value in the longitudinal direction.
$V_1=JK(x_2)/n$, Darcy's velocity parallel to the bedding.
V_2 vertical drift velocity.
U mean velocity field in the horizontal direction.
$\mathbf{X}=(x_1, x_2)$ coordinate vector.
x_1, x_2 spatial coordinates, respectively parallel and normal to the bedding.
$\mathbf{X}=\mathbf{X}(t, a)$, trajectory of a solute particle, whose coordinates along x_1, x_2 are X_1, X_2.
$\mathbf{X}'=\mathbf{X} - \mathbf{U}t$, deviation of actual trajectory from mean value.
X_{11} two-particle covariance of the displacement of at time t.
$\alpha=a/l$, dimensionless initial position of the particle.
Δt time step of the numerical simulation.
$\xi_K(r)=\int_0^r \rho_K(r')\, dr'$, auxiliary function.
$\lambda=L/I$, dimensionless initial size of the solute body.
$\rho_X(r)$ autocorrelation function of the random field X.
σ_X^2 variance of the random field X.
$\tau=V_2 t/l$, dimensionless time.
$\langle\ \rangle$ statistical expectation.
Var ( ) variance of a random function.

Acknowledgments. This note is a spinoff of a project undertaken by a study group within the Summer School on Environmental Dynamics organized jointly by the Istituto Veneto di Scienze Lettere ed Arti and the Italian National Research Council and held at Venice in the summer of 1990. The participants in the working group, besides the authors, were Brune Brunone (Italy), Georgia Destouni (Sweden), Luigi Fraccarollo (Italy), Joao-Paulo Lobo Ferreira (Portugal), Alberto Marinelli (Italy), and Hernan Quinodoz (Argentina). The authors wish to thank the anonymous reviewers for their thorough reading of the paper and their constructive criticism.

REFERENCES

Aris, R., On the dispersion of a solute in a fluid flowing through a tube, *Proc. R. Soc. London, Ser. A*, *235*, 67–77, 1956.
Black, T. C., and D. L. Freyberg, Stochastic modeling of vertically averaged concentration uncertainty in a perfectly stratified aquifer, *Water Resour. Res.*, *23*, 997–1004, 1987.
Cvetkovic, V. D., and A. M. Shapiro, Solute advection in stratified formations, *Water Resour. Res.*, *25*, 1283–1290, 1989.
Dagan, G., *Flow and Transport in Porous Formations*, Springer-Verlag, New York, 1989.
Dagan, G., Transport in heterogeneous porous formations: Spatial moments, ergodicity and effective dispersion, *Water Resour. Res.*, *26*, 1281–1290, 1990.
Dagan, G., On transport in formations of large heterogeneity scales, in *Proceedings International Conference on Transport and Mass Exchange in Sand and Gravel Aquifers*, in press, 1991.
Gelhar, L. W., A. L. Gutjahr, and R. L. Naff, Stochastic analysis of macrodispersion in a stratified aquifer, *Water Resour. Res.*, *15*, 1387–1397, 1979.
Güven, O., and F. J. Molz, Deterministic and stochastic analysis of dispersion in an unbounded stratified porous medium, *Water Resour. Res.*, *22*, 156–164, 1986.
Güven, O., F. J. Molz, and J. G. Melville, An analysis of dispersion in a stratified aquifer, *Water Resour. Res.*, *20*, 1337–1354, 1984.
Kitanidis, P. K., Prediction by the method of moments of transport in a heterogeneous formation, *J. Hydrol.*, *102*, 453–473, 1988.
Marle, C., P. Simandoux, J. Pacsirsky, and C. Gaulier, Etude du déplacement de fluides miscibles en milieu poreux stratifié, *Rev. Inst. Fr. Pet.*, *22*, 272–294, 1967.
Matheron, G., and G. de Marsily, Is transport in porous media always diffusive? A counterexample, *Water Resour. Res.*, *16*, 901–917, 1980.
Mercado, A., The spreading pattern of injected water in a permeability stratified aquifer, *IAHS AISH Publ.*, *72*, 23–36, 1967.
Taylor, G. I., Dispersion of soluble matter in solvent flowing slowly through a tube, *Proc. R. Soc. London, Ser. A*, *219*, 186–203, 1953.

G. Dagan, Department of Fluid Mechanics and Heat Transfer, Faculty of Engineering, Tel Aviv University, Ramat Aviv, 69978 Tel Aviv, Israel.
A. Rinaldo, Dipartimento di Ingegneria Civile e Ambientale, Università di Trento, Mesiano di Povo, I-38050 Trento, Italy.
P. Salandin, Istituto di Idraulica "Giovanni Poleni," Università di Padova, via Loredan 20, I-35131 Padova, Italy.

(Received February 18, 1991;
revised July 5, 1991;
accepted July 19, 1991.)